CWI

Centrum voor Wiskunde en Informatica
Centre for Mathematics and Computer Science

E.D. de Goede

Finite difference methods for the three-dimensional
hydrodynamic equations

Finite difference methods for the three–dimensional hydrodynamic equations

Erik D. de Goede

Centre for Mathematics and Computer Science
P.O.Box 4079, 1009 AB Amsterdam, The Netherlands

A three-dimensional hydrodynamic sea model is formulated using Cartesian coordinates in the horizontal and both Cartesian and depth-following (sigma) coordinates in the vertical. For a linear test model the stability and efficiency on vector computers of various time integrators is compared for a wind induced flow in a rectangular basin having dimensions representing the North Sea.

1. Introduction

In this report one-step time integrators for the three-dimensional hydrodynamic equations which describe motion of a sea are developed and compared with each other with respect to stability and efficiency on vector computers. In Section 2 the hydrodynamic equations are given in both Cartesian and depth-following (sigma) coordinates. The equations describe the motion, the elevation and the transport of salt and heat of water. However, in this report we confine ourselves to a simplified, linear model, which is described in Section 3.

In Section 4 the system of partial differential equations (PDEs) is converted into a system of ordinary differential equations (ODEs) by discretization of the space derivatives by second order finite differences. This is the so-called method of lines. In Section 5 various time integrators are developed for this system of ODEs. Application of time integrators for a three-dimensional model requires extensive computation. Especially for fully implicit methods, this is a severe disadvantage. If an explicit method is used, then besides the C.F.L. stability condition there is also a condition imposed by the vertical diffusion term [1]. In many problems the last condition is more restrictive. To investigate how this condition influences the stability, we test time integrators which are explicit, semi-implicit or implicit in the vertical. In the numerical experiments, which are described in Section 6, a wind induced test model is used. This model has been used by others [1,3] and is consequently an ideal case for comparing the results. For the time integrator which performs at best in our experiments, we will carry out a stability analysis, which is described in Section 7. It appears that the stability condition is only slightly dependent of the vertical mesh size Δz. Thus, the time step is limited only in terms of the horizontal mesh sizes, not by the vertical mesh size. Moreover, on a vector computer (viz., a 2-pipe CDC Cyber 205) it appears that this method requires even less computational effort then the explicit method tested in the experiments.

2. Mathematical formulation

2.1 Mathematical model in Cartesian coordinates

In this section a three-dimensional hydrodynamic sea model will be presented. The following symbols are used :

A^x, A^y	horizontal diffusion coefficients for momentum
A^z	vertical diffusion coefficient for momentum
C	Chezy's coefficient
D^x, D^y	horizontal diffusion coefficients for heat/salinity
D^z	vertical diffusion coefficient for heat/salinity
f	Coriolis term
F_b	bottom stress in x-direction
F_s	surface stress in x-direction
g	acceleration due to gravity
G_b	bottom stress in y-direction
G_s	surface stress in y-direction
h	undisturbed depth of water
H	$= h + \zeta$
p	pressure
p_a	atmospheric pressure
s	salinity
t	time
T	temperature
x, y, z	a right-handed set of Cartesian coordinates
u, v, w	velocity components in x,y,z-direction in Cartesian coordinates
WF	wind stress
φ	angle between wind direction and the positive x-axis
ρ	density of water
ρ_o	reference density (a constant)
$\Delta\rho$	density variation ($= \rho - \rho_o$)
σ	vertical coordinate after sigma transformation
$\tau_{xx}, \tau_{xy}, \dots$	components of the stress tensor
ω	vertical velocity in sigma coordinates
ζ	elevation above undisturbed depth.

The equations of horizontal motion for an incompressible nonhomogeneous source-free fluid in Cartesian coordinates with the z-axis positive upward may be written as [2]

$$\frac{\partial u}{\partial t} = -\frac{\partial(uu)}{\partial x} - \frac{\partial(uv)}{\partial y} - \frac{\partial(uw)}{\partial z} + fv + \frac{1}{\rho}\left\{ -\frac{\partial p}{\partial x} + \frac{\partial\tau_{xx}}{\partial x} + \frac{\partial\tau_{xy}}{\partial y} + \frac{\partial\tau_{xz}}{\partial z} \right\} \qquad (2.1)$$

$$\frac{\partial v}{\partial t} = -\frac{\partial(vu)}{\partial x} - \frac{\partial(vv)}{\partial y} - \frac{\partial(vw)}{\partial z} - fu + \frac{1}{\rho}\left\{ -\frac{\partial p}{\partial y} + \frac{\partial\tau_{yx}}{\partial x} + \frac{\partial\tau_{yy}}{\partial y} + \frac{\partial\tau_{yz}}{\partial z} \right\} . \qquad (2.2)$$

In estuarine and coastal flow systems, the fluid motions are predominantly horizontal. The vertical acceleration of the large scale motion is extremely small, particularly if compared

with the acceleration by gravity. Therefore, neglecting the vertical acceleration and advection is justified, and the equation of motion in the vertical becomes the hydrostatic equation

$$\frac{\partial p}{\partial z} + \rho g = 0 \ . \quad (2.3)$$

The equation of continuity is

$$\frac{\partial u}{\partial x} + \frac{\partial v}{\partial y} + \frac{\partial w}{\partial z} = 0 \ . \quad\quad\quad (2.4)$$

The equations of salt and heat balance are

$$\frac{\partial s}{\partial t} = -\frac{\partial (su)}{\partial x} - \frac{\partial (sv)}{\partial y} - \frac{\partial (sw)}{\partial z} + \frac{\partial\left(D^x \frac{\partial s}{\partial x}\right)}{\partial x} + \frac{\partial\left(D^y \frac{\partial s}{\partial y}\right)}{\partial y} + \frac{\partial\left(D^z \frac{\partial s}{\partial z}\right)}{\partial z} \quad (2.5)$$

$$\frac{\partial T}{\partial t} = -\frac{\partial (Tu)}{\partial x} - \frac{\partial (Tv)}{\partial y} - \frac{\partial (Tw)}{\partial z} + \frac{\partial\left(D^x \frac{\partial T}{\partial x}\right)}{\partial x} + \frac{\partial\left(D^y \frac{\partial T}{\partial y}\right)}{\partial y} + \frac{\partial\left(D^z \frac{\partial T}{\partial z}\right)}{\partial z} \ , \quad (2.6)$$

and the equation of state

$$\rho = \rho_0 + \Delta\rho(s,T) \ , \quad\quad\quad (2.7)$$

with $\Delta\rho(s,T)$ a function specifying the variations in the density.

Three generally applied assumptions are included in equations (2.1) to (2.7) :

i)   The curvature effects of the earth are neglected. The earth's rotation is modelled by a constant Coriolis parameter f.

ii)   The variations of the density are not taken into account in the continuity equation (2.4). This simplification causes that the water, although not homogeneous, is incompressible.

iii)   The pressure effect on the density is neglected (isothermal compressibility). Due to this simplification, the density depends only on the salinity and temperature.

In the equation for the heat balance (2.6) we use the same diffusion coefficients as in the equation for salt balance (2.5). The components of the stress tensor in (2.1) and (2.2) can be expressed as gradients of Reynolds stresses [2], through the relationships

$$\tau_{xx} = A^x \frac{\partial u}{\partial x}, \quad \tau_{xy} = A^y \frac{\partial u}{\partial y}, \quad \tau_{xz} = A^z \frac{\partial u}{\partial z} \ ,$$

$$\tau_{yx} = A^x \frac{\partial v}{\partial x}, \quad \tau_{yy} = A^y \frac{\partial v}{\partial y}, \quad \tau_{yz} = A^z \frac{\partial v}{\partial z}.$$

The internal pressure distribution in the flow can be derived by vertical integration of equation (2.3), which leads to

$$\text{at } z = h_1 : \quad\quad p = p_a + \rho_0 g(\zeta - h_1) + g \int_{h_1}^{\zeta} \Delta\rho \ dz \ ,$$

Applying Leibnitz' rule on the derivatives of an integral

$$\frac{\partial}{\partial \eta} \int_{h_1}^{\zeta} f \, dz = \int_{h_1}^{\zeta} \frac{\partial f}{\partial \eta} dz + f(\zeta) \frac{\partial \zeta}{\partial \eta} - f(h_1) \frac{\partial h_1}{\partial \eta} \; ,$$

where f stands for $\Delta \rho$ and η for x or y. Thus, we obtain for the pressure gradients at $z = h_1$

$$\frac{\partial p}{\partial x} = \rho g \frac{\partial(\zeta - h_1)}{\partial x} + g \int_{h_1}^{\zeta} \frac{\partial \rho}{\partial x} dz \qquad \text{and} \qquad \frac{\partial p}{\partial y} = \rho g \frac{\partial(\zeta - h_1)}{\partial y} + g \int_{h_1}^{\zeta} \frac{\partial \rho}{\partial y} dz \; .$$

The variations of the atmospheric pressure p_a are small compared to the variations of $\rho g(\zeta - h_1)$ and have been neglected.

It is also assumed that a particle which is on the surface must remain on it; This assumption is satisfied if

$$\text{at } z = \zeta(x,y,t) \quad : \quad w = \frac{d\zeta}{dt} = u \frac{\partial \zeta}{\partial x} + v \frac{\partial \zeta}{\partial y} + \frac{\partial \zeta}{\partial t} . \tag{2.8}$$

A similar condition applies at the bottom :

$$\text{at } z = -h(x,y) \quad : \quad w = u \frac{\partial(-h)}{\partial x} + v \frac{\partial(-h)}{\partial y} \; . \tag{2.9}$$

The change of the surface level ζ is related to the vertically integrated flow. Integrating the continuity equation (2.4) from the bottom to the surface, gives

$$w(x,y,\zeta,t) - w(x,y,-h,t) = - \int_{-h}^{\zeta} \frac{\partial u}{\partial x} dz - \int_{-h}^{\zeta} \frac{\partial v}{\partial y} dz \; . \tag{2.10}$$

Then, applying Leibnitz' rule and combination of (2.10) with (2.8) and (2.9), leads to

$$\frac{\partial \zeta}{\partial t} = - \frac{\partial}{\partial x} \int_{-h}^{\zeta} u \, dz - \frac{\partial}{\partial y} \int_{-h}^{\zeta} v \, dz \; .$$

Note that we now have a depth integrated equation, which also occurs in two-dimensional models [11]. Similarly, by integrating from the bottom to a certain level $z=h_1$, we obtain a relationship for the vertical velocity w :

$$w(x,y,h_1,t) = - \frac{\partial}{\partial x} \int_{-h}^{h_1} u \, dz - \frac{\partial}{\partial y} \int_{-h}^{h_1} v \, dz + u \frac{\partial(h_1)}{\partial x} + v \frac{\partial(h_1)}{\partial y} \; . \tag{2.11}$$

This expression for w allows a non-zero normal velocity at the bottom (see (2.9)). However, another possible boundary condition is

at z = -h(x,y)   :   w = 0 ,

requiring that the normal velocity component vanishes at the bottom. This condition can be obtained by neglecting the last two terms in the right-hand side of (2.11). Similarly, the condition

at z = -h(x,y)   :   u = v = 0 ,

yields that the tangent velocity component vanishes at the bottom.

To conclude this section, we summarize the three-dimensional hydrodynamic equations in Cartesian coordinates :

$$\frac{\partial u}{\partial t} = -\frac{\partial (uu)}{\partial x} - \frac{\partial (uv)}{\partial y} - \frac{\partial (uw)}{\partial z} + fv + \frac{1}{\rho}\left\{ -\frac{\partial p}{\partial x} + \frac{\partial\left(A^x\frac{\partial u}{\partial x}\right)}{\partial x} + \frac{\partial\left(A^y\frac{\partial u}{\partial y}\right)}{\partial y} + \frac{\partial\left(A^z\frac{\partial u}{\partial z}\right)}{\partial z} \right\} \tag{2.12}$$

$$\frac{\partial v}{\partial t} = -\frac{\partial (vu)}{\partial x} - \frac{\partial (vv)}{\partial y} - \frac{\partial (vw)}{\partial z} - fu + \frac{1}{\rho}\left\{ -\frac{\partial p}{\partial y} + \frac{\partial\left(A^x\frac{\partial v}{\partial x}\right)}{\partial x} + \frac{\partial\left(A^y\frac{\partial v}{\partial y}\right)}{\partial y} + \frac{\partial\left(A^z\frac{\partial v}{\partial z}\right)}{\partial z} \right\} \tag{2.13}$$

$$w = -\frac{\partial}{\partial x}\int_{-h}^{h_1} u\, dz - \frac{\partial}{\partial y}\int_{-h}^{h_1} v\, dz \tag{2.14}$$

$$\frac{\partial \zeta}{\partial t} = w(\zeta) = -\frac{\partial}{\partial x}\int_{-h}^{\zeta} u\, dz - \frac{\partial}{\partial y}\int_{-h}^{\zeta} v\, dz \tag{2.15}$$

$$\frac{\partial s}{\partial t} = -\frac{\partial (su)}{\partial x} - \frac{\partial (sv)}{\partial y} - \frac{\partial (sw)}{\partial z} + \frac{\partial\left(D^x\frac{\partial s}{\partial x}\right)}{\partial x} + \frac{\partial\left(D^y\frac{\partial s}{\partial y}\right)}{\partial y} + \frac{\partial\left(D^z\frac{\partial s}{\partial z}\right)}{\partial z} \tag{2.16}$$

$$\frac{\partial T}{\partial t} = -\frac{\partial (Tu)}{\partial x} - \frac{\partial (Tv)}{\partial y} - \frac{\partial (Tw)}{\partial z} + \frac{\partial\left(D^x\frac{\partial T}{\partial x}\right)}{\partial x} + \frac{\partial\left(D^y\frac{\partial T}{\partial y}\right)}{\partial y} + \frac{\partial\left(D^z\frac{\partial T}{\partial z}\right)}{\partial z} \tag{2.17}$$

$$\rho = \rho_0 + \Delta\rho(s,T) \tag{2.18}$$

$$\frac{\partial p}{\partial x} = \rho g\frac{\partial(\zeta-h_1)}{\partial x} + g\int_{h_1}^{\zeta}\frac{\partial p}{\partial x}dz \qquad \text{and} \qquad \frac{\partial p}{\partial y} = \rho g\frac{\partial(\zeta-h_1)}{\partial y} + g\int_{h_1}^{\zeta}\frac{\partial p}{\partial y}dz \ , \tag{2.19}$$

with $-h \leq h_1 \leq \zeta$.

The boundary condition at the sea surface $z = \zeta$ for the vertical diffusion term is given by

$$\left(A^z\frac{\partial u}{\partial z}\right)_\zeta = F_s , \qquad \left(A^z\frac{\partial v}{\partial z}\right)_\zeta = G_s . \qquad (2.20)$$

Similarly, the boundary condition at the bottom $z = -h(x,y)$ is given by

$$\left(A^z\frac{\partial u}{\partial z}\right)_{-h} = F_b , \qquad \left(A^z\frac{\partial v}{\partial z}\right)_{-h} = G_b . \qquad (2.21)$$

The bottom stress is parametrized using a linear law of bottom friction, of the form

$$F_b = g\rho u_d / C^2, \qquad G_b = g\rho v_d / C^2,$$

with u_d and v_d the components of the current at some depth near the bottom. The wind stresses are expressed as

$$F_s = WF \cos \varphi, \qquad G_s = WF \sin \varphi.$$

2.2 Mathematical model in sigma coordinates

The domain in which the equations of Section 2.1 have to be solved, changes in time because the sea surface ζ is time-dependent. To enable the domain to be constant in time, the equations have to be transformed in the vertical direction into depth-following (sigma) coordinates [8]. Transforming equations (2.12) to (2.19) from the interval $-h \leq z \leq \zeta$ into the constant interval $1 \geq \sigma \geq 0$, using the so-called sigma transformation

$$\sigma = \frac{\zeta-z}{h+\zeta} \qquad \left(= \frac{\zeta-z}{H}\right) ,$$

gives

$$\frac{\partial u}{\partial t} = -\frac{\partial(uu)}{\partial x} - \frac{\partial(uv)}{\partial y} - \frac{\partial(u\omega)}{\partial\sigma} + fv + \frac{1}{\rho}\left\{ -\frac{\partial p}{\partial x} + \frac{\partial\left(A^x\frac{\partial u}{\partial x}\right)}{\partial x} + \frac{\partial\left(A^y\frac{\partial u}{\partial y}\right)}{\partial y} + \frac{1}{H^2}\frac{\partial\left(A^z\frac{\partial u}{\partial\sigma}\right)}{\partial\sigma} \right\} \qquad (2.22)$$

$$\frac{\partial v}{\partial t} = -\frac{\partial(vu)}{\partial x} - \frac{\partial(vv)}{\partial y} - \frac{\partial(v\omega)}{\partial\sigma} - fu + \frac{1}{\rho}\left\{ -\frac{\partial p}{\partial y} + \frac{\partial\left(A^x\frac{\partial v}{\partial x}\right)}{\partial x} + \frac{\partial\left(A^y\frac{\partial v}{\partial y}\right)}{\partial y} + \frac{1}{H^2}\frac{\partial\left(A^z\frac{\partial v}{\partial\sigma}\right)}{\partial\sigma} \right\} \qquad (2.23)$$

$$\omega = \frac{1}{H}\left\{ -(1-\sigma)\left(\frac{\partial}{\partial x}(H\int_0^1 u\,d\sigma) + \frac{\partial}{\partial y}(H\int_0^1 v\,d\sigma)\right) + \frac{\partial}{\partial x}(H\int_\sigma u\,d\sigma) + \frac{\partial}{\partial y}(H\int_\sigma v\,d\sigma) \right\} \qquad (2.24)$$

$$\frac{\partial \zeta}{\partial t} = -\frac{\partial}{\partial x}(H \int_0^1 u d\sigma) - \frac{\partial}{\partial y}(H \int_0^1 v d\sigma) \tag{2.25}$$

$$\frac{\partial s}{\partial t} = -\frac{\partial(su)}{\partial x} - \frac{\partial(sv)}{\partial y} - \frac{\partial(sw)}{\partial z} + \frac{\partial \left(D^x \frac{\partial s}{\partial x}\right)}{\partial x} + \frac{\partial \left(D^y \frac{\partial s}{\partial y}\right)}{\partial y} + \frac{1}{H^2} \frac{\partial \left(D^z \frac{\partial s}{\partial \sigma}\right)}{\partial \sigma} \tag{2.26}$$

$$\frac{\partial T}{\partial t} = -\frac{\partial(Tu)}{\partial x} - \frac{\partial(Tv)}{\partial y} - \frac{\partial(Tw)}{\partial z} + \frac{\partial \left(D^x \frac{\partial T}{\partial x}\right)}{\partial x} + \frac{\partial \left(D^y \frac{\partial T}{\partial y}\right)}{\partial y} + \frac{1}{H^2} \frac{\partial \left(D^z \frac{\partial T}{\partial \sigma}\right)}{\partial \sigma} \tag{2.27}$$

$$\frac{\partial p}{\partial x} = \rho g \, \sigma \frac{\partial H}{\partial x} - gH \int_\sigma^0 \frac{\partial \rho}{\partial x} d\sigma \qquad \text{and} \qquad \frac{\partial p}{\partial y} = \rho g \, \sigma \frac{\partial H}{\partial y} - gH \int_\sigma^0 \frac{\partial \rho}{\partial y} d\sigma . \tag{2.28}$$

The relation between the new vertical velocity ω and the old velocity w is given by

$$\omega = \frac{1}{H}\left\{ -w + (1-\sigma) \frac{\partial \zeta}{\partial t} + u(\frac{\partial \zeta}{\partial x} - \sigma \frac{\partial H}{\partial x}) + v(\frac{\partial \zeta}{\partial y} - \sigma \frac{\partial H}{\partial y}) \right\}.$$

Transforming surface and sea-bed boundary conditions (2.20) and (2.21) to sigma coordinates, gives at the sea surface

$$-\left(A^z \frac{\partial u}{\partial \sigma}\right)_0 = H F_s , \qquad -\left(A^z \frac{\partial v}{\partial \sigma}\right)_0 = H G_s , \tag{2.29}$$

and at the bottom $z = -h(x,y)$

$$-\left(A^z \frac{\partial u}{\partial z}\right)_1 = H F_b , \qquad -\left(A^z \frac{\partial v}{\partial z}\right)_1 = H G_b . \tag{2.30}$$

3. Test model

In the remainder of this report we will consider the simplified, linearized three-dimensional test model in sigma coordinates

$$\frac{\partial u}{\partial t} = fv - g\frac{\partial \zeta}{\partial x} + \frac{1}{\rho}\frac{1}{h^2} \frac{\partial \left(A^z \frac{\partial u}{\partial \sigma}\right)}{\partial \sigma} \tag{3.1}$$

$$\frac{\partial v}{\partial t} = -fu - g\frac{\partial \zeta}{\partial y} + \frac{1}{\rho}\frac{1}{h^2} \frac{\partial \left(A^z \frac{\partial v}{\partial \sigma}\right)}{\partial \sigma} \tag{3.2}$$

$$\frac{\partial \zeta}{\partial t} = - \frac{\partial}{\partial x} (h \int_0^1 u d\sigma) - \frac{\partial}{\partial y} (h \int_0^1 v d\sigma) , \qquad (3.3)$$

with boundary conditions (2.29) and (2.30) and ρ constant. In the next section we will explain why we have chosen the sigma coordinates. This test model, which has been used by others [1,3], can be derived from the sigma transformed equations (2.22) to (2.28) by :

a)   omitting the advective terms,
b)   omitting the horizontal diffusion terms,
c)   simplifying the pressure term by

$$\sigma \frac{\partial H}{\partial x} = \sigma \frac{\partial (\zeta - z)}{\sigma \partial x} = \frac{\partial (\zeta - z)}{\partial x} \approx \frac{\partial \zeta}{\partial x} \qquad \text{(analogous } \sigma \frac{\partial H}{\partial y} \text{)} ,$$

d)   replacing H by h in the continuity equation and in the equations of motion,
e)   omitting the equations of salt and heat balance.

4. Space discretization

In this section the space discretization of equations (3.1) to (3.3) is developed using finite differences in both horizontal and vertical direction. For the three-dimensional finite differences there are essentially two approaches in the vertical (see Section 2.1 and 2.2). In the model with Cartesian coordinates, a fixed grid is used in the vertical, through which the fluid is free to move. This can be visualized by considering the fluid in horizontal slices, in which only the upper layer has a time-variable height. This approach has been developed by Leendertse and Liu [6]. Since this model is fixed in the vertical, the number of grid layers increases as the depth increases, but reduces in shallow regions. This problem of reduced vertical resolution in the shallow regions can be overcome by using the depth-following (sigma) coordinates of Section 2.2. Then, a constant number of grid layers is used in the vertical at each horizontal grid point. Moreover, there are no 'zig-zag boundaries' in the vertical in the case of an irregular bottom. From a computational point of view, it is advantageous to have a constant number of grid layers too, especially on vector computers. Therefore, we choose sigma coordinates.

The computational domain is covered by an $nx \cdot ny \cdot ns$ rectangular grid.

The notation used for the velocities is $U_{i,j,k}$ and $V_{i,j,k}$, where i,j refers to the horizontal grid point and k to the vertical layer. The surface elevation points are denoted by $Z_{i,j}$ and are specified at the sea surface. The diffusion coefficients are assumed to vary only through the vertical. Hence, A_k refers to the coefficient at layer k.

In the horizontal a staggered grid is used (see Fig. 1a). At the upper layer only, $Z_{i,j}$ is computed at grid points denoted by O.

The use of a staggered grid has the following advantages :
a) For the system of equations (3.1) to (3.3) the storage requirements decrease with a factor four (the mesh sizes of the staggered grid in Fig. 1a are twice the mesh sizes of the unstaggered grid). However, components that are not available in a particular grid point, have to be obtained by averaging.
b) It simplifies the boundary conditions (e.g., in a U-boundary points no conditions for the V-velocity have to be prescribed).
c) It reduces the possibility of spurious "2Δx-waves" [10].

In the vertical a varying mesh of thickness $\Delta\sigma_k$, where k refers to the k-th grid layer from the surface, is used (see Fig. 1b). Hence, it is possible to increase the resolution near the surface and the bottom.
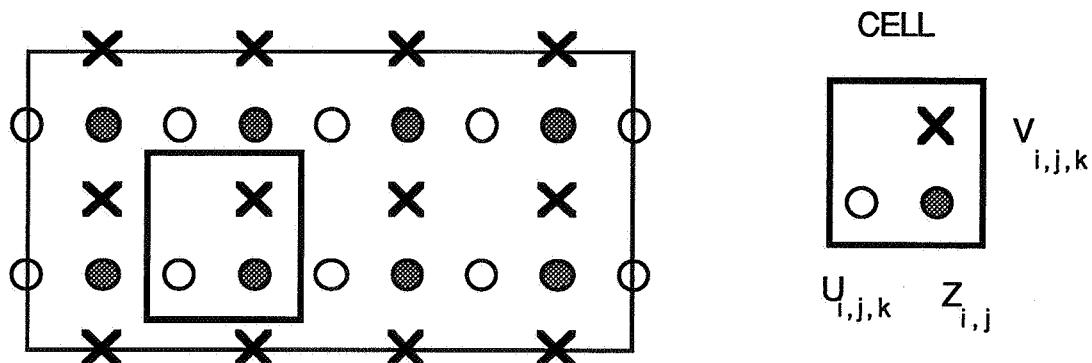

Fig. 1a.   Staggered grid in (x,y)-plane.
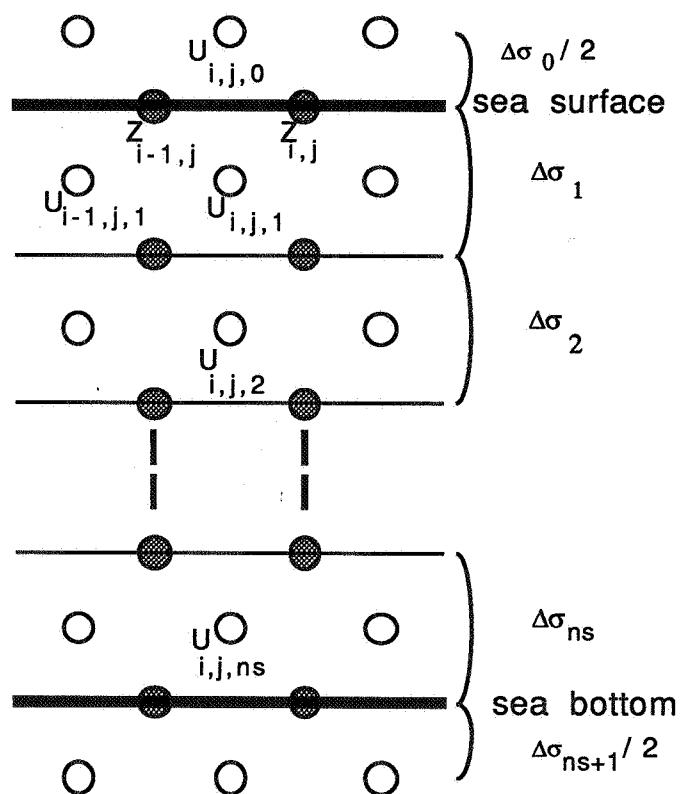
Fig. 1b.   Staggered grid in (x,σ)-plane.

In the (y,σ)-plane the staggering is identical as in Fig. 1b.

For the approximation of the spatial derivatives, second order central differences are used in both the horizontal and vertical direction. The horizontal mesh sizes are denoted by Δx and Δy. Now, for the equations of motion (3.1) and (3.2), we obtain

$$\frac{\partial U_{i,j,k}}{\partial t} = f \, \tilde{V}_{i,j,k} - g \left(\frac{Z_{i+1,j} - Z_{i,j}}{\Delta x} \right)$$

$$+ \frac{1}{\rho} \frac{1}{d_{i,j}^2} \frac{1}{\Delta \sigma_k} \left\{ \frac{A_{k+1}(U_{i,j,k+1} - U_{i,j,k})}{0.5(\Delta \sigma_{k+1} + \Delta \sigma_k)} - \frac{A_k(U_{i,j,k} - U_{i,j,k-1})}{0.5(\Delta \sigma_k + \Delta \sigma_{k-1})} \right\} , \qquad (4.1)$$

$$\frac{\partial V_{i,j,k}}{\partial t} = - f \tilde{U}_{i,j,k} - g \left(\frac{Z_{i,j+1} - Z_{i,j}}{\Delta y} \right)$$

$$+ \frac{1}{\rho} \frac{1}{e_{i,j}^2} \frac{1}{\Delta \sigma_k} \left\{ \frac{A_{k+1}(V_{i,j,k+1} - V_{i,j,k})}{0.5(\Delta \sigma_{k+1} + \Delta \sigma_k)} - \frac{A_k(V_{i,j,k} - V_{i,j,k-1})}{0.5(\Delta \sigma_k + \Delta \sigma_{k-1})} \right\} , \qquad (4.2)$$

where $\quad \tilde{V}_{i,j,k} = 0.25 \cdot \left(V_{i,j,k} + V_{i,j-1,k} + V_{i-1,j,k} + V_{i-1,j-1,k} \right) ,$

$\tilde{U}_{i,j,k} = 0.25 \cdot \left(U_{i,j,k} + U_{i+1,j,k} + U_{i,j+1,k} + U_{i+1,j+1,k} \right) ,$

$d_{i,j} = 0.5 \cdot \left(h((i+1)\Delta x, j\Delta y) + h(i\Delta x, j\Delta y) \right) \quad$ and

$e_{i,j} = 0.5 \cdot \left(h(i\Delta x, (j+1)\Delta y) + h(i\Delta x, j\Delta y) \right).$

To satisfy the boundary conditions (2.29) and (2.30), it is necessary to introduce fictitious grid points above the surface and below the sea bed (see Fig. 1b). Assuming that $\Delta \sigma_0 = \Delta \sigma_1$, the boundary conditions are given by

$$-A_1 \frac{U_{i,j,1} - U_{i,j,0}}{\Delta \sigma_1} = d_{i,j} F_s , \qquad -A_1 \frac{V_{i,j,1} - V_{i,j,0}}{\Delta \sigma_1} = e_{i,j} G_s .$$

$$-A_{ns+1} \frac{U_{i,j,ns+1} - U_{i,j,ns}}{\Delta \sigma_{ns}} = d_{i,j} F_b , \qquad -A_{ns+1} \frac{V_{i,j,ns+1} - V_{i,j,ns}}{\Delta \sigma_{ns}} = e_{i,j} G_b ,$$

It should be noted that the fictitious grid points have been introduced only to describe the boundary conditions and are not used in the computations.

Considering equation (3.3), we have to approximate an integral which extends from the bottom to the surface. The vertical direction has been divided into a number of grid layers (see Fig 1b). Let s_k denote the interfaces between the layers, defined by

$$s_k = \sum_{q=1}^{k} \Delta \sigma_q , \quad k=0,\dots,ns .$$

Then, for the integral in equation (3.3) we can write

$$\int_0^1 u(i\Delta x, j\Delta y)ds = \sum_{k=1}^{ns} \int_{s_{k-1}}^{s_k} u(i\Delta x, j\Delta y)ds \approx \sum_{k=1}^{ns}(s_k - s_{k-1})U_{i,j,k} = \sum_{k=1}^{ns}\Delta\sigma_k U_{i,j,k} \ ,$$

which leads to

$$\frac{\partial Z_{i,j}}{\partial t} = -\frac{1}{\Delta x}\left\{ d_{i+1,j}\sum_{k=1}^{ns}\Delta\sigma_k U_{i+1,j,k} - d_{i,j}\sum_{k=1}^{ns}\Delta\sigma_k U_{i,j,k}\right\}$$

$$-\frac{1}{\Delta y}\left\{ e_{i,j+1}\sum_{k=1}^{ns}\Delta\sigma_k V_{i,j+1,k} - e_{i,j}\sum_{k=1}^{ns}\Delta\sigma_k V_{i,j,k}\right\} . \qquad (4.3)$$

Now, the semi-discretized system (4.1) to (4.3) can be written in the form

$$\frac{d}{dt}\begin{pmatrix}U\\V\\Z\end{pmatrix} = \begin{pmatrix}\Lambda_{\sigma\sigma} & F & -g\Theta_2 D_x \\ -F & \Lambda_{\sigma\sigma} & -g\Theta_2 D_y \\ -\Theta_1(h_x + hD_x) & -\Theta_1(h_y + hD_y) & 0 \end{pmatrix}\begin{pmatrix}U\\V\\Z\end{pmatrix}, \qquad (4.4)$$

with U and V grid functions approximating the velocities u and v, with components $U_{i,j,k}$ and $V_{i,j,k}$ (the components are numbered lexicographically),

$\Lambda_{\sigma\sigma}$ a tridiagonal matrix approximating the vertical diffusion term,

Θ_1 a $(nx \cdot ny \cdot ns) \cdot (nx \cdot ny)$ matrix,

Θ_2 a $(nx \cdot ny) \cdot (nx \cdot ny \cdot ns)$ matrix,

F a four diagonal matrix (due to the grid staggering) of order $(nx \cdot ny \cdot ns)^2$ approximating the Coriolis term,

h_x and h_y diagonal matrices of order $(nx \cdot ny)^2$ approximating $\partial h/\partial x$ and $\partial h/\partial y$ and

D_x and D_y bidiagonal matrices of order $(nx \cdot ny)^2$ approximating the differential operators $\partial/\partial x$ and $\partial/\partial y$, respectively.

E.g., in the case of ns = 4, the structure of system (4.4), in which the four diagonal matrix F is replaced by a diagonal matrix, is

$$\frac{d}{dt}\begin{pmatrix} U \\ V \\ Z \end{pmatrix} = \begin{pmatrix} \boxed{\diagdown} & \boxed{\diagdown} & \boxed{\diagdown} \\ \boxed{\diagdown} & \boxed{\diagdown} & \boxed{\diagdown} \\ \boxed{\diagdown} & \boxed{\diagdown} & \square \end{pmatrix}\begin{pmatrix} U \\ V \\ Z \end{pmatrix}$$
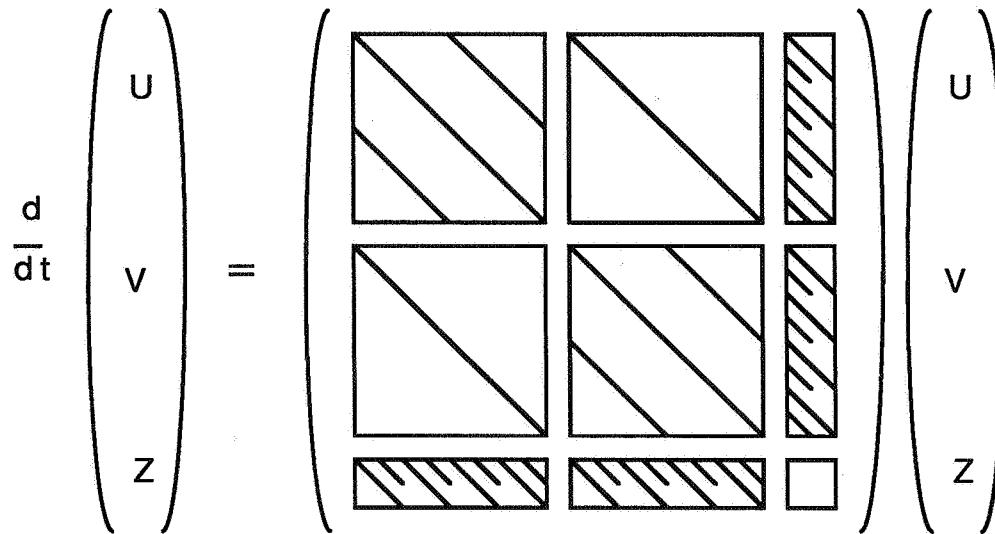
Fig. 2.

5. Time integration

In this section one-step time integrators for the semi-discretized system (4.4) are described. We will introduce time integrators which are explicit, semi-implicit or implicit in the vertical direction.

Considering explicit methods, we do not use the Forward Euler method, since the stability region of this method does not contain any part of the imaginary axis. Therefore, we apply the one-step, explicit, 3-stage, second order Runge-Kutta method which has an imaginary stability boundary $\beta = 2$. Let the system of ODEs

$$\frac{dS}{dt} = f(t, S(t))$$

represent the semi-discretized system (4.4), with $S = (U,V,Z)^T$ and $f(t,S(t))$ denoting the right-hand side of (4.4). Then, the Runge-Kutta method can be written in the form

$$\begin{aligned} S_1 &= S^n \\ S_2 &= S^n + 0.5\tau\, f(t_n, S_1) \\ S_3 &= S^n + 0.5\tau\, f(t_n + 0.5\tau, S_2) \\ S^{n+1} &= S^n + \tau\, f(t_n + 0.5\tau, S_3) \, , \end{aligned} \tag{5.1}$$

where n denotes the time level $n\tau$, with τ the time step. It is known that the imaginary stability boundary of method (5.1) is optimal for explicit, 3-stage, second order Runge-Kutta methods [4].

On the other hand, the (first order) Backward Euler method for system (4.4) reads

$$\begin{pmatrix} I - \tau\Lambda_{\sigma\sigma} & -\tau F & \tau g\Theta_2 D_x \\ \tau F & I - \tau\Lambda_{\sigma\sigma} & \tau g\Theta_2 D_y \\ \tau\Theta_1(h_x+hD_x) & \tau\Theta_1(h_y+hD_y) & I \end{pmatrix} \begin{pmatrix} U^{n+1} \\ V^{n+1} \\ Z^{n+1} \end{pmatrix} = \begin{pmatrix} U^n \\ V^n \\ Z^n \end{pmatrix}. \tag{5.2}$$

This method requires extensive computation, since at each time step a linear system of order $(2nx \cdot ny \cdot ns + nx \cdot ny)^2$ has to be solved. To reduce the computational complexity the following simplifications can be made :

a) uncouple the computation of the **Z** velocity from the computation of the **U-V** velocities. This leads to

$$\begin{pmatrix} I - \tau\Lambda_{\sigma\sigma} & -\tau F & \tau g\Theta_2 D_x \\ \tau F & I - \tau\Lambda_{\sigma\sigma} & \tau g\Theta_2 D_y \\ 0 & 0 & I \end{pmatrix} \begin{pmatrix} U^{n+1} \\ V^{n+1} \\ Z^{n+1} \end{pmatrix} = \begin{pmatrix} I & 0 & 0 \\ 0 & I & 0 \\ -\tau\Theta_1(h_x+hD_x) & -\tau\Theta_1(h_y+hD_y) & I \end{pmatrix} \begin{pmatrix} U^n \\ V^n \\ Z^n \end{pmatrix} \tag{5.3}$$

or

$$\begin{pmatrix} I - \tau\Lambda_{\sigma\sigma} & -\tau F & 0 \\ \tau F & I - \tau\Lambda_{\sigma\sigma} & 0 \\ \tau\Theta_1(h_x+hD_x) & \tau\Theta_1(h_y+hD_y) & I \end{pmatrix} \begin{pmatrix} U^{n+1} \\ V^{n+1} \\ Z^{n+1} \end{pmatrix} = \begin{pmatrix} I & 0 & -\tau g\Theta_2 D_x \\ 0 & I & -\tau g\Theta_2 D_y \\ 0 & 0 & I \end{pmatrix} \begin{pmatrix} U^n \\ V^n \\ Z^n \end{pmatrix}. \tag{5.3a}$$

Due to the coupling of the velocity components, we do not use methods (5.3) and (5.3a) in our experiments.

b) Moreover, we may uncouple the computation of the **U** velocity from the **V** velocity by transferring a Coriolis term to the right-hand side. Thus, for method (5.3) we obtain

$$\begin{pmatrix} I - \tau\Lambda_{\sigma\sigma} & 0 & \tau g\Theta_2 D_x \\ \tau F & I - \tau\Lambda_{\sigma\sigma} & \tau g\Theta_2 D_y \\ 0 & 0 & I \end{pmatrix} \begin{pmatrix} U^{n+1} \\ V^{n+1} \\ Z^{n+1} \end{pmatrix} = \begin{pmatrix} I & \tau F & 0 \\ 0 & I & 0 \\ -\tau\Theta_1(h_x+hD_x) & -\tau\Theta_1(h_y+hD_y) & I \end{pmatrix} \begin{pmatrix} U^n \\ V^n \\ Z^n \end{pmatrix} \tag{5.4}$$

and for method (5.3a)

$$\begin{pmatrix} I - \tau\Lambda_{\sigma\sigma} & 0 & 0 \\ \tau F & I - \tau\Lambda_{\sigma\sigma} & 0 \\ \tau\Theta_1(h_x+hD_x) & \tau\Theta_1(h_y+hD_y) & I \end{pmatrix} \begin{pmatrix} U^{n+1} \\ V^{n+1} \\ Z^{n+1} \end{pmatrix} = \begin{pmatrix} I & \tau F & -\tau g\Theta_2 D_x \\ 0 & I & -\tau g\Theta_2 D_y \\ 0 & 0 & I \end{pmatrix} \begin{pmatrix} U^n \\ V^n \\ Z^n \end{pmatrix}. \tag{5.4a}$$

The methods can be made more symmetric in various ways. In the experiments we observed that symmetrization of the **Z** component deteriorated the stability considerably. Therefore, we will only symmetrize the velocity components. Thus, the symmetrical variant of method (5.4a) reads

$$\begin{pmatrix} I-0.5\tau\Lambda_{\sigma\sigma} & 0 & 0 \\ \tau F & I-0.5\tau\Lambda_{\sigma\sigma} & 0 \\ \tau\Theta_1(h_x+hD_x) & \tau\Theta_1(h_y+hD_y) & I \end{pmatrix} \begin{pmatrix} U^{n+1} \\ V^{n+1} \\ Z^{n+1} \end{pmatrix} = \begin{pmatrix} I+0.5\tau\Lambda_{\sigma\sigma} & \tau F & -\tau g\Theta_2 D_x \\ 0 & I+0.5\tau\Lambda_{\sigma\sigma} & -\tau g\Theta_2 D_y \\ 0 & 0 & I \end{pmatrix} \begin{pmatrix} U^n \\ V^n \\ Z^n \end{pmatrix} \tag{5.5}$$

Methods (5.4) and (5.4a) can be made more explicit by transferring the Coriolis term to the right-hand side. For method (5.4), this leads to

$$
\begin{pmatrix}
I-\tau\Lambda_{\sigma\sigma} & 0 & \tau g\Theta_2 D_x \\
0 & I-\tau\Lambda_{\sigma\sigma} & \tau g\Theta_2 D_y \\
0 & 0 & I
\end{pmatrix}
\begin{pmatrix}
U^{n+1} \\
V^{n+1} \\
Z^{n+1}
\end{pmatrix}
=
\begin{pmatrix}
I & \tau F & 0 \\
-\tau F & I & 0 \\
-\tau\Theta_1(h_x+hD_x) & -\tau\Theta_1(h_y+hD_y) & I
\end{pmatrix}
\begin{pmatrix}
U^n \\
V^n \\
Z^n
\end{pmatrix}
\quad (5.6)
$$

Considering methods (5.4) to (5.6), nx·ny tridiagonal linear systems (of order ns) have to be solved each time step. For the solution of the tridiagonal systems we use the sequential Gaussian Elimination method. The sequential steps are performed for the nx·ny systems at the same time, thus resulting in vector operations of length nx·ny and consequently a good performance.

A further simplification can be achieved by splitting $\Lambda_{\sigma\sigma}$ into $\Lambda_L+\Lambda_U$, with Λ_L a lower bidiagonal matrix and Λ_U an upper bidiagonal matrix. Then, we obtain

$$
\begin{pmatrix}
I-\tau\Lambda_L & 0 & \tau g\Theta_2 D_x \\
0 & I-\tau\Lambda_L & \tau g\Theta_2 D_y \\
0 & 0 & I
\end{pmatrix}
\begin{pmatrix}
U^{n+1} \\
V^{n+1} \\
Z^{n+1}
\end{pmatrix}
=
\begin{pmatrix}
I+\tau\Lambda_U & \tau F & 0 \\
-\tau F & I+\tau\Lambda_U & 0 \\
-\tau\Theta_1(h_x+hD_x) & -\tau\Theta_1(h_y+hD_y) & I
\end{pmatrix}
\begin{pmatrix}
U^n \\
V^n \\
Z^n
\end{pmatrix}
. \quad (5.7)
$$

In the next time step the matrices Λ_L and Λ_U are interchanged. So, the direction of the sweep is alternated every time step to avoid any bias in the method. This scheme has been developed by Davies for the solution of the same test problem [1].

6. Numerical experiments

To compare the various time integrators we choose a test problem which has been used by others [1,3]. In this experiment the water is initially at rest and the motion in the basin is generated by a constant wind stress. The closed rectangular basin has dimensions representative of the North Sea. Thus, a wind driven circulation is gradually developed and finally reaches a steady state. The following parameters are used in this experiment :

L = 400 km
Δx = 400/9 km
B = 800 km
Δy = 800/17 km
f = 0.44/3600 = 1.22 e-4
g = 9.81 [m/s^2]
h = 65 m
A^z = 0.065/ρ
WF = 1.5 [kg m/s^2] (= 15 [dyn/cm^2])
ρ = 1025 [kg/m^3]
φ = 90 [deg.] (= northerly wind) .

It is evident from Fig. 1b that the **U** and **V** grid points do not coincide with the sea surface or the sea bed. To compute surface currents we interpolate from grid points of the upper two layers in a linear way :

$$U_{i,j,surface} = U_{i,j,1} - \Delta\sigma_1 \left(\frac{U_{i,j,2} - U_{i,j,1}}{\Delta\sigma_1 + \Delta\sigma_2} \right)$$

In a similar way the surface currents for the V-velocity can be obtained.

We integrate over a period of 24 hours, with time steps of 3, 5, 10, 15, 20 and 30 minutes. The experiments have been carried out on a (2-pipe) CDC Cyber 205. Tables 6.1 and 6.2 show the water elevation computed at the south-western corner of the basin for two different vertical resolutions, namely $\Delta\sigma = 1/ns$, with $ns = 5$ and $ns = 25$. We do not list the surface currents, because they show a similar behaviour as the surface elevations. Overflow is denoted by ***.

The methods used in this experiment are :
>   the 3-stage Runge-Kutta method (5.1)
>   the vertically semi-implicit method (5.7)
>   the vertically implicit method (5.6)
>   the vertically implicit method (5.4)
>   the vertically implicit method (5.4a)
>   the symmetrized, vertically implicit method (5.5).

Table 6.1 shows that the results are comparable for all methods when $ns = 5$. However, in the case of 25 layers the methods behave differently. The RK3 method becomes unstable for already the smallest time step used in this experiment. Method (5.7), in which bidiagonal systems have to be solved, gives accurate solutions for time steps of maximal five minutes. However, the vertically implicit methods behave as in the case of five layers. In both cases the maximal time step is about 20 minutes. This suggests that for these methods the maximal stable time step is more or less independent of the vertical mesh size. In the next section we will carry out a stability analysis for method (5.4a). Although the differences are small among these vertically implicit methods, methods (5.4a) and (5.5) behave slightly better, especially when we look at the times at which the elevation ζ reaches its maximum or minimum. So, it is advantageous to evaluate the equations of motion before the continuity equation.

For these methods, firstly the **U** component is computed, then the **V** component and finally the **Z** component. Since the components are computed after each other, this is very advantageous for the storage requirements.

Concerning computation time, it is evident that both methods are very efficient on vector computers. It is surprising that the vertically implicit methods are slightly more efficient than method (5.7), in which bidiagonal systems have to be solved. This is due to the way of programming. The tridiagonal systems are build up and solved at the same time. This leads to a smaller number of divisions. In general, the efficiency of both methods will be comparable.

7. Stability analysis

In this section the stability of method (5.4a) is studied. For that purpose we introduce the eigenvalues $i\delta_x$, $i\delta_y$ and $\gamma_{\sigma\sigma}$ of the difference operators D_x, D_x and $\Lambda_{\sigma\sigma}$, corresponding to the eigenvectors $e^{i(\alpha_1 \Delta x + \alpha_2 \Delta y + \alpha_3 \Delta\sigma)}$. The following assumptions are made :

Table 6.1 : Surface elevations with ns = 5

method	Δt (min.)	ζ_{max} (cm)	time (hrs)	ζ_{min} (cm)	time (hrs)	ζ(end) (cm)	comp. time (sec.)
(5.1)	3	172.6	8.7	45.8	18.3	103.9	4.36
	5	172.6	8.7	45.8	18.3	104.0	2.61
	10	172.3	8.7	45.9	18.3	104.0	1.31
	15	172.0	8.7	46.3	18.3	103.9	0.87
	20	171.6	8.7	46.6	18.3	103.9	0.65
	30	* * *					
(5.7)	3	172.5	8.7	45.8	18.3	103.9	1.34
	5	172.5	8.7	45.8	18.3	103.8	0.80
	10	172.5	8.8	45.6	18.3	103.7	0.40
	15	172.8	8.7	45.0	18.3	103.6	0.27
	20	173.4	8.7	44.4	18.3	103.6	0.20
	30	* * *					
(5.6)	3	172.7	8.7	45.5	18.3	103.8	1.26
	5	172.7	8.7	45.4	18.3	103.8	0.75
	10	172.9	8.8	44.8	18.3	103.7	0.38
	15	173.2	9.0	43.8	18.3	103.5	0.25
	20	174.0	9.0	42.6	18.3	103.6	0.19
	30	* * *					
(5.4)	3	173.0	8.8	45.5	18.3	103.8	1.26
	5	173.3	8.7	45.3	18.4	103.7	0.76
	10	173.7	8.7	44.8	18.5	103.4	0.38
	15	175.0	9.0	44.1	18.5	102.9	0.25
	20	175.0	9.0	44.0	18.7	102.6	0.19
	30	* * *					
(5.4a)	3	173.0	8.7	45.5	18.3	104.0	1.26
	5	173.3	8.7	45.3	18.3	104.0	0.75
	10	174.1	8.7	44.8	18.3	104.0	0.38
	15	175.0	8.7	44.1	18.3	103.9	0.25
	20	176.1	8.7	43.2	18.3	104.1	0.19
	30	* * *					
(5.5)	3	172.9	8.7	45.6	18.3	104.0	1.53
	5	173.2	8.7	45.5	18.3	104.1	0.92
	10	173.8	8.7	45.1	18.3	104.1	0.46
	15	174.6	8.7	44.4	18.3	104.1	0.31
	20	175.7	8.7	44.0	18.3	104.3	0.23
	30	* * *					

Table 6.2 : Surface elevations with ns = 25

method	Δt (min.)	ζ_{max} (cm)	time (hrs)	ζ_{min} (cm)	time (hrs)	ζ(end) (cm)	comp. time (sec.)
(5.1)	3	* * *					
(5.7)	3	173.5	8.6	41.1	18.2	104.1	5.05
	5	174.1	8.6	40.6	18.2	104.6	3.03
	10	179.4	8.3	34.1	17.8	108.0	1.51
	15	191.7	8.3	16.7	17.9	115.1	1.01
	20	212.1	8.0	-3.1	18.3	130.8	0.76
	30	* * *					
(5.6)	3	173.4	8.8	41.0	18.3	103.8	4.36
	5	173.5	8.8	40.8	18.3	103.8	2.58
	10	173.7	8.7	40.2	18.3	103.7	1.29
	15	173.9	8.8	39.3	18.5	103.5	0.86
	20	174.7	9.0	37.9	18.3	103.6	0.65
	30	* * *					
(5.4)	3	173.8	8.8	41.0	18.3	103.8	4.31
	5	174.1	8.8	40.8	18.4	103.7	2.59
	10	174.8	8.8	40.3	18.5	103.4	1.29
	15	175.8	9.0	39.5	18.5	102.8	0.86
	20	176.9	9.0	38.7	18.7	102.5	0.65
	30	* * *					
(5.4a)	3	173.8	8.7	41.0	18.3	104.0	4.30
	5	174.1	8.7	40.8	18.3	104.1	2.58
	10	174.8	8.7	40.3	18.3	104.1	1.29
	15	175.8	8.7	39.5	18.3	103.9	0.86
	20	176.9	8.7	38.7	18.3	104.1	0.65
	30	* * *					
(5.5)	3	173.7	8.7	41.1	18.3	104.0	5.79
	5	174.0	8.7	40.9	18.3	104.1	3.47
	10	174.7	8.7	40.6	18.3	104.1	1.74
	15	175.4	8.7	39.9	18.3	104.1	1.16
	20	176.5	8.7	39.4	18.3	104.3	0.87
	30	* * *					

a) $h_x = h_y = 0$ (constant bottom) ,

b) $\sum\limits_{k=1}^{ns} \Delta\sigma_k \tau (h_x + hD_x) U_{i,j,k} = \tau(h_x + hD_x)\, U_{i,j}$.

c) $\forall k : 1 \le k \le ns : \Delta\sigma_k = 1/ns$.

Although assumption b) reduces the analysis to a two-dimensional stability analysis, the results are in agreement with our three-dimensional experiments. We construct for method (5.4a) the so-called amplification matrix [9]. Then, the amplification matrix can be written as

$$G = A^{-1}\, B ,$$

where

$$A = \begin{pmatrix} I - \tau\gamma_{\sigma\sigma} & 0 & 0 \\ \tau F & I - \tau\gamma_{\sigma\sigma} & 0 \\ i\tau h\delta_x & i\tau h\delta_y & I \end{pmatrix} \quad B = \begin{pmatrix} I & \tau F & -i\tau g\delta_x \\ 0 & I & -i\tau g\delta_y \\ 0 & 0 & I \end{pmatrix} ,$$

with

$$\delta_x = \frac{\sin(\alpha_1\, 0.5\Delta x)}{0.5\Delta x}, \quad \delta_y = \frac{\sin(\alpha_2\, 0.5\Delta y)}{0.5\Delta y} \quad \text{and} \quad \gamma_{\sigma\sigma} = \frac{-2+\cos(\alpha_3\Delta\sigma)}{(\Delta\sigma)^2}\frac{A^\sigma}{\rho h^2} , \tag{7.1}$$

where α_1, α_2 and α_3 are constants. Stability in the sense of O'Brien-Hyman-Kaplan [7] is ensured if $\|G\| \le 1$. To study the stability we write

$$
\begin{aligned}
G &= q \quad q^{-1} A^{-1} q \quad q^{-1} B q \quad q^{-1} && \Leftrightarrow \\
G &= q \, (q^{-1} A q)^{-1} \, (q^{-1} B q) \, q^{-1} && \Leftrightarrow \\
G &= q \quad \tilde{A}^{-1} \qquad \tilde{B} \qquad q^{-1}
\end{aligned}
$$

where

$$q = \begin{pmatrix} 1 & 0 & 0 \\ 0 & 1 & 0 \\ 0 & 0 & \sqrt{\dfrac{h}{g}} \end{pmatrix} ,$$

and

$$\tilde{A} = \begin{pmatrix} I - \tau\gamma_{\sigma\sigma} & 0 & 0 \\ \tau F & I - \tau\gamma_{\sigma\sigma} & 0 \\ i\tau\tilde{\delta}_x & i\tau\tilde{\delta}_y & I \end{pmatrix} \quad \text{and} \quad \tilde{B} = \begin{pmatrix} I & \tau F & -i\tau\tilde{\delta}_x \\ 0 & I & -i\tau\tilde{\delta}_y \\ 0 & 0 & I \end{pmatrix} ,$$

with

$$\tilde{\delta}_x = \sqrt{gh}\,\frac{\sin(\alpha_1\,0.5\Delta x)}{0.5\Delta x}\,, \qquad \tilde{\delta}_y = \sqrt{gh}\,\frac{\sin(\alpha_2\,0.5\Delta y)}{0.5\Delta y}\,.$$

In the remainder of the section we will omit the tildes. Now, suppose that λ are the eigenvalues of G. Then, the eigenvalues satisfy

$$\det\left|A^{-1}B - \lambda I\right| = 0 \qquad \Leftrightarrow$$

$$\det\left|A^{-1}\right| \cdot \det\left|B - \lambda A\right| = 0\,.$$

Assuming that A is invertible, we find

$$\det\left|B - \lambda A\right| = \det\begin{vmatrix} I+\lambda(\tau\gamma_{\sigma\sigma}-1) & \tau F & -i\tau\delta_x \\ -\lambda\tau F & I+\lambda(\tau\gamma_{\sigma\sigma}-1) & -i\tau\delta_y \\ -i\lambda\tau\delta_x & -i\lambda\tau\delta_y & I-\lambda \end{vmatrix} = 0\,. \tag{7.2}$$

The eigenvalue equation for G is

$$\lambda^3 + a_1\lambda^2 + a_2\lambda + a_3 = 0\,,$$

where

$$a_1 = -\frac{(\tau\gamma_{\sigma\sigma} - 3 + \tau^2\delta_y^2)(\tau\gamma_{\sigma\sigma} - 1) - \tau^2 F^2 + \tau^3\delta_x\delta_y F + \tau^2\delta_x^2(\tau\gamma_{\sigma\sigma} - 1)}{(1-\tau\gamma_{\sigma\sigma})^2}$$

$$a_2 = -\frac{2\tau\gamma_{\sigma\sigma} - 3 + \tau^2\delta_y^2 + \tau^2 F^2 + \tau^2\delta_x^2 - \tau^3\delta_x\delta_y F}{(1-\tau\gamma_{\sigma\sigma})^2}$$

$$a_3 = -\frac{1}{(1-\tau\gamma_{\sigma\sigma})^2}\,.$$

Note that the coefficients are real, whereas the matrix in (7.2) is complex. Therefore, we can apply the Hurwitz-criterion [5] to ensure that the eigenvalues of the amplification matrix G are within the unit circle. Thus, we must require

$$1 + a_1 + a_2 + a_3 > 0$$
$$1 - a_1 + a_2 - a_3 > 0$$
$$3 + a_1 - a_2 - 3a_3 > 0$$
$$1 - a_2 + a_1 a_3 - a_3^2 > 0\,.$$

We obtain the following inequalities :

(a) $\tau^3\gamma_{\sigma\sigma} (\delta_x^2 + \delta_y^2) < 0$

(b) $\tau^2\gamma_{\sigma\sigma}^2 - 4\tau\gamma_{\sigma\sigma} + 4 + \tau^2(\delta_x^2 + \delta_y^2) (0.5\tau\gamma_{\sigma\sigma} - 1) + \tau^3\delta_x\delta_y F - \tau^2 F^2 > 0$

(c) $\tau^2\gamma_{\sigma\sigma}^2 + \tau^2(\delta_x^2 + \delta_y^2) (2 - \tau\gamma_{\sigma\sigma}) - 2\tau^3\delta_x\delta_y F + 2\tau^2 F^2 > 0$

(d) $\tau^3\gamma_{\sigma\sigma}^3 - 2\tau^2\gamma_{\sigma\sigma}^2 + \tau\gamma_{\sigma\sigma} (\tau^2\delta_x^2 + \tau^2\delta_y^2 - \tau^3\delta_x\delta_y F + \tau^2 F^2) - 2\tau^2 F^2 + 2\tau^3\delta_x\delta_y F < 0$.

From (7.1) it can be easily seen that $\gamma_{\sigma\sigma} < 0$. Thus, inequality (a) can not be satisfied if $\delta_x = \delta_y = 0$. However, in that case the amplification matrix is of the simple form

$$G = \begin{pmatrix} I+\lambda(\tau\gamma_{\sigma\sigma}-1) & \tau F & 0 \\ -\lambda\tau F & I+\lambda(\tau\gamma_{\sigma\sigma}-1) & 0 \\ 0 & 0 & I-\lambda \end{pmatrix},$$

with the eigenvalues $\lambda = 1, \dfrac{-\tau^2 F^2 - 2(\tau\gamma_{\sigma\sigma} - 1) \pm \tau F \sqrt{\tau^2 F^2 + 4(\tau\gamma_{\sigma\sigma} - 1)}}{2(\tau\gamma_{\sigma\sigma} - 1)^2}$.

So, inequality (a) can be rewritten to

(a') $\dfrac{-\tau^2 F^2 - 2(\tau\gamma_{\sigma\sigma} - 1) \pm \tau^2 F \sqrt{\tau^2 F^2 + 4(\tau\gamma_{\sigma\sigma} - 1)}}{2(\tau\gamma_{\sigma\sigma} - 1)^2} \leq 1$.

The inequalities (a'), (b), (c) and (d) are too complicated to derive stability conditions. Therefore, we neglect the influence of the Coriolis term. Then, it can be verified that inequalities (a'), (c) and (d) are always satisfied. For the second inequality we obtain :

$$\tau < \frac{1}{\sqrt{gh}} \frac{0.5}{\sqrt{\frac{1}{\Delta^2 x} + \frac{1}{\Delta^2 y}}} \sqrt{4 + \frac{2\tau}{\Delta^2\sigma} \frac{A^\sigma}{\rho h^2}} . \tag{7.3}$$

This condition shows that the maximal time step is more or less independent of $\Delta\sigma$. Moreover, as the vertical diffusion coefficient increases, the maximal time step increases. For the parameters used in our experiment, stability condition (7.3) yields a maximal stable time step of about 1300 seconds, which is in agreement with the results. Experimentally, we observe that the maximal stable time step is of the same order when the Coriolis term is not neglected.

8. Conclusions

In this report one-step time integrators for the three-dimensional hydrodynamic equations have been presented and analyzed. Due to the large system of equations containing many terms, we experimented a lot with the order of computation of the various components. From our linear test problem, it appeared to be advantageous to :
a)   treat the vertical diffusion term implicitly,
b)   compute the velocity components before the elevation component,
c)   treat the Coriolis term as implicit as possible.
This are three characteristics of methods (5.4a) and (5.5). Moreover, on a vector computer, these methods appeared to be as efficient as explicit methods.
In future, among others, methods (5.4a) and (5.5) will be examined for nonlinear test problems.

9.   References

[1]   A.M. DAVIES, Application of the DuFort-Frankel and Saul'ev methods with time splitting to the formulation of a three dimensional hydrodynamic sea model, *Intern. J. Numer. Meth.ods Fluids*, **5** (1985), 405-425.
[2]   DELFT HYDRAULICS LABORATORY, *Three-dimensional circulation models for shallow lakes and seas*, Report R 900 I, 1976.
[3]   N.S. HEAPS, *On the numerical solution of the three-dimensional hydrodynamic equations for tides and storm surges,* Mem. Soc. Roy. Sci. Liege Ser. 6, **2** (1972), 143-180.
[4]   P.J. VAN DER HOUWEN, *Construction of integration formulas for initial-value problems*, North-Holland, Amsterdam, 1977.
[5]   J.D. LAMBERT, *Computational methods in ordinary differential equations*, John Wiley & Sons, London, 1973.
[6]   J.J. LEENDERTSE, R.C. ALEXANDER AND S.-K. LIU, *A three dimensional model for estuaries and coastral seas : volume I, Principles of computation*, The Rand Corporation, RM-1417-OWRR, 1973.
[7]   G.G. O'BRIEN, M.A. HYMAN AND S. KAPLAN, A study of the numerical solution of partial defferential equations, *J.   Mathematics Phys.*, **29** (1950), 223-251.
[8]   N.A. PHILLIPS, A coordinate system having some special advantages for numerical forcasting, *J. Meteorol.*, **14** (1957), 184-194.
[9]   R.D. RICHTMYER AND K.W. MORTON, *Difference methods for initial value problems*, Interscience Publishers, Wiley, New York, London.
[10]   G.S. STELLING, *On the construction of computational methods for shallow water flow problems*, Thesis, TU Delft, Delft, 1983.
[11]   F.W. WUBS, *Numerical solution of the shallow-water equations*, Thesis, Centre for Mathematics and Computer Science, Amsterdam, 1987.